

Interactions of ultrathin Pb films with Ru(0001) and Pd(111)

G. Liu, K. A. Davis, D. C. Meier, P. S. Bagus,* and D. W. Goodman*

Department of Chemistry, Texas A&M University, P.O. Box 30012, College Station, Texas 77842-3012, USA

G. W. Zajac

BP Chemicals Company, 150 West Warrenville Road, P.O. Box 3011, Naperville, Illinois 60566-7011 USA

(Received 24 April 2003; published 2 July 2003)

The interaction of ultrathin Pb films with Ru(0001) and Pd(111) has been studied with x-ray photoelectron spectroscopy (XPS) and thermal desorption spectroscopy (TDS). XPS and TDS show that at room temperature Pb grows on Ru(0001) via a Stranski-Krastanov mechanism, i.e., after completion of the first adlayer of Pb on Ru(0001), further Pb deposition leads to the formation of three-dimensional islands. Upon annealing to 500 K, the overlayer Pb undergoes significant clustering with the extent dictated by the initial coverages. XPS results show that the Pb $4f_{7/2}$ core level binding energy (BE) increases slightly (+0.3 eV) as the Pb coverage increases from 0.07 ML to multilayers. When the first monolayer of Pb/Ru(0001) has been completed, the Pb $4f_{7/2}$ BE has nearly reached the BE value for bulk Pb; it is only 0.1 eV lower. At ~ 2 ML, the Pb $4f_{7/2}$ BE is equivalent to that of bulk Pb. In contrast, at room temperature, Pb alloys with the Pd(111) surface, the Pd $3d_{5/2}$ BE increasing ~ 0.8 eV with coverage from 0.07- to 4.3-ML Pb. The Pb $4f_{7/2}$ BEs also increase with increasing coverage reaching the bulk value of Pb at a coverage of ~ 2 ML. The Pb $4f_{7/2}$ BE at 0.07 ML is 0.55 eV smaller than that of bulk Pb. The lineshape and position of the x-ray induced Pd Auger features ($M_{4,5}VV$) also display significant changes upon alloying. For Pb/Pd alloys, annealing to 500 K does not induce further changes in the Pd ($M_{4,5}VV$) Auger features. The core level BE shifts are discussed in terms of possible initial and final state contributions. In particular, the initial state BE shift mechanisms of hybridization and environmental conduction band charge density are explained in the context of prior theoretical studies. It is shown that $6s \rightarrow 6p$ hybridization in Pb can be expected to be sufficiently large to contribute to the observed BE shifts.

DOI: 10.1103/PhysRevB.68.035406

PACS number(s): 68.35.-p, 82.80.Pv, 78.30.Er, 68.55.Jk

I. INTRODUCTION

Bimetallic surfaces exhibit a variety of interesting physical and chemical properties,¹ especially as compared to surfaces composed of the individual components of the bimetallic system. One of the principal goals of bimetallic studies is to better understand the unique function of these mixed-metal surfaces in heterogeneous catalysts. When characterizing traditional bimetallic catalysts, it is often difficult to determine the nature of the various phases in highly dispersed metal particles. Thus, surface science techniques and model bimetallic catalysts (thin films and/or alloys) have been used frequently to simplify the studies of “real world” catalysts. During the past 10 years, significant attention has been directed to correlating the heteronuclear metal-metal bond properties with the electronic/catalytic properties of bimetallic surfaces.²⁻⁵ For many of these studies, refractory metal substrates such as Ta, Mo, Ru, Re, and W, have been chosen to study overlayer phases of metals such as Pd, Cu, and Ni. Recently, Pd alloying with sp metals like Cu has received attention because of the superior properties of Pd/Cu as an industrial catalyst; here, a particular interest is understanding the mutual influences that the additive and the host have on each other.⁶ Among a variety of surface science techniques, x-ray photoelectron spectroscopy (XPS) has been utilized most often to study core level binding energy (BE) shifts since these shifts may provide information about the electronic perturbations of the individual components of the bimetallic systems. One of our major purposes in the present paper is to show that substantial caution must be used in the

interpretation of core level BE shifts.^{7,8} In particular, this is true for analyses in terms of charge transfer, between the individual components. Theoretical studies, see for example Refs. 7 and 8, have shown that there are competing physical mechanisms which act to shift the BE in opposite directions. As we shall describe in more detail in Sec. 4, the origin of surface core level shifts (SCLSs), has been decomposed into contributions from different physical mechanisms^{7,8} and two canceling initial state mechanisms have been quantified for the Cu(100) surface. One mechanism, arising from the presence of the conduction band charge density, contributes ~ -0.5 eV to the SCLS while the second, arising from the $3d$ hybridization, contributes $\sim +1.2$ eV to the SCLS. A positive sign for the SCLS contribution indicates that this contribution favors a larger BE for a bulk than for a surface atom. Note that these two contributions are of roughly comparable magnitude and that they are canceling to reduce the total SCLS. The cancellation of approximately equal large shifts may make it difficult to assign the origin of an observed total shift, especially without detailed theoretical studies for the systems of interest. In this paper, we present compelling evidence that such studies will be needed in order to make definitive interpretations of the BE shifts. While it would be desirable to have these interpretations, it is very important to be aware that over-simplified, possibly incorrect, analyses of the BE shifts must be used with caution.

Palladium is a material used in a variety of practical catalytic processes; see, for example, Refs. 9 and 10. Furthermore, in order to improve selectivity for certain hydrogenation reactions,¹¹⁻¹³ a second sp metal, often Pb, is used as an

additive.^{11–17} Previous XPS studies directed toward understanding practical catalysts for these hydrogenation processes^{11–13,15–17} have shown that it is difficult to determine the nature of bimetallic surfaces formed with Pb and Pd. These difficulties are due to the heterogeneity of conventional supported catalysts and to the diverse catalyst preparation methods. In the catalysts studied, more or less separated phases, including monometallic Pb, Pb/Pd alloys, and Pb oxides, can coexist with one phase being coated or partially covered by the other. Consequently, the role of Pb in altering hydrogenation in Pb/Pd catalysts is still not well understood. The addition of trace amounts of Pb improves the performance of Pd containing catalysts for various oxidation reactions; see, for example, Refs. 18 and 19. On the other hand, the presence of Pb can also drastically decrease the activity of a Pd containing catalyst.²⁰ Although possible mechanisms have been suggested for these promoting¹⁹ or poisoning²⁰ effects of Pb addition, better understanding of the reactions would be helpful.

In the present paper, the interactions between Pb and Ru(0001) and Pd(111) single crystals have been investigated in order to better understand these bimetallic surfaces. Ru was chosen because no intermetallic compounds are known to exist between Pb and Ru.²¹ XPS is employed to investigate the nature of the bimetallic bond, with particular emphasis on the Pb growth modes and the nature of the Pb electronic perturbation in an overlayer or alloy phase.

II. EXPERIMENTAL DETAILS

The experiments were performed in an ultrahigh vacuum system, described in detail elsewhere.²² The base pressure of the chamber was less than 2×10^{-10} Torr. The system consists of two interconnected chambers, one for thermal desorption spectroscopy (TDS) and sample preparation, and the other for electron spectroscopy using a Kratos XSA M800 hemispherical electron energy analyzer and a twin-anode x-ray gun (unmonochromatized Mg $K\alpha$ radiation was used for this study). The XPS data were recorded at an angle of 30° with respect to the sample normal to enhance surface sensitivity. The spectrometer was operated in a fixed-analyzer transition mode with a pass energy of 38 eV. The core level binding energies were calibrated with respect to Cu and Au surfaces and referenced to the Fermi level.

Pb (99.999%, Aldrich Chemical Company, Inc.) was evaporated from a high purity ceramic crucible, which was heated resistively by W coils. The Pb source was extensively outgassed prior to use and monitored by a mass spectrometer mounted in line-of-sight in order to ensure a constant flux of lead.

The Ru(0001) and Pd(111) single crystals were polished following standard polishing procedures. The samples were mounted on tantalum leads and heated resistively. The crystal temperature was monitored with a W-5%Re/W-26%Re thermocouple spot-welded to the edge of the crystal. The sample was cleaned in vacuum by several cycles of argon ion bombardment and annealing until no contamination was detected by XPS.

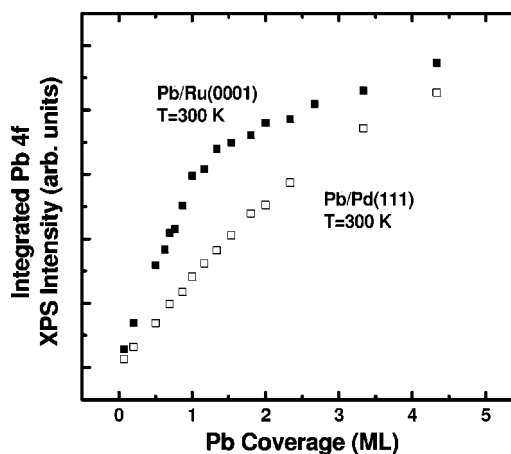


FIG. 1. Variation of the Pb 4*f* intensity as a function of Pb deposition amount on Ru(0001) and Pd(111) at room temperature.

III. RESULTS

The Pb coverage (film thickness) was calibrated by depositing incremental amounts of Pb on Ru(0001) and Pd(111) at room temperature and monitoring the XPS Pb 4*f* photoemission peaks following each dose. Plots of the intensity of the Pb 4*f* XPS peaks as a function of Pb coverage on Ru(0001) and on Pd(111) are given in Fig. 1; the calibration of the coverage is explained below. For both Pb/Ru(0001) and Pb/Pd(111), the Pb XPS signal initially increases linearly with Pb deposition time. For Pb on Ru(0001), the well-defined break in the slope is assumed to correspond to completion of the first Pb monolayer (ML). It is also apparent that beyond the monolayer point, further deposition continues to increase the Pb intensity but without additional break points. This is consistent with the onset of three-dimensional cluster formation after the first monolayer since no alloys of Pb and Ru are known.²¹

For Pb deposition on Pd(111), the Pb XPS intensity shows no noticeable breaks, and is markedly less intense than that from Pb/Ru(0001). Because the surface atom densities for Ru(0001) and Pd(111) are 1.64×10^{15} atoms/cm² and 1.54×10^{15} atoms/cm², respectively, the intensity difference between Pb on Ru and Pb on Pd is not due to the packing density differences between Pb/Ru and Pb/Pd. Thus, the lower XPS intensity for Pb/Pd(111) than for Pb/Ru(0001) may be a result of a different growth mode for Pb on Pd(111) than on Ru(0001). Two growth modes for Pb on Pd(111) may be able to explain the lower XPS Pb 4*f* intensities: (i) alloying of Pb with Pd and (ii) nucleation of 3D Pb crystallites. Of course, both of these growth modes could be present.

The Pb coverage was independently calibrated by TDS after depositing Pb on clean Ru. Figure 2 shows a family of TDS spectra of Pb deposited at room temperature on Ru(0001) as a function of coverage. At the highest coverages, two desorption features are well resolved: (i) a high-temperature feature at ~ 1075 K becomes more intense and is saturated after a 1300-s exposure; and (ii) a low-temperature feature (~ 635 K) that begins to grow after 1300 s. The Pb exposure at the initial appearance of this second feature, assigned to desorption of multilayer Pb, correlates

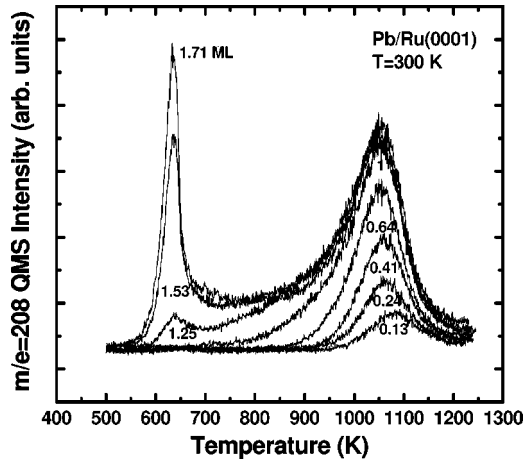


FIG. 2. Evolution of the TDS spectra of Pb deposited at room temperature onto Ru(0001) as a function of the deposition amount. The spectra were acquired with a linear heating rate of 5 K/s.

with the break point in the XPS plot of Fig. 1. In all work to follow, we shall denote the amount of Pb deposited in units of coverage. Based on the XPS break point and TPD for Pd/Ru(0001), we define 1-ML coverage as equivalent to a 1300 s exposure, making the assumption that the sticking coefficient is nearly unity at all Pb coverages on Pd(111) and Ru(0001). It is noteworthy that in the submonolayer range, the desorption maximum at ~ 1075 K shifts to lower temperature by ~ 25 K with increasing coverage up to 1 ML and then becomes constant.

The low-temperature feature is characteristic of zero-order desorption kinetics, whereas the high-temperature peak is characteristic of first-order kinetics.²³ For zero-order desorption, the activation energy, E_d , for the low-temperature feature using an Arrhenius relationship is 130 kJ/mol, a value significantly smaller than the heat of sublimation for bulk Pb (~ 196 kJ/mol).²⁴ The estimated activation energies for desorption, using a Redhead approximation²³ and assuming first-order desorption with a prefactor of 10^{13} s⁻¹, for Pb coverages of 0.13, 0.41, and 1 ML, are 286, 281, and 278 kJ/mol, respectively. These values are similar, changing by only 3% between 0.13 and 1 ML, and considerably larger than the heat of sublimation of bulk Pb (by $\sim 45\%$). It is reasonable³ to take this larger activation energy as a strong indication that the Pb-Ru bond is significantly stronger than the Pb-Pb bond.

Figure 3 shows XPS spectra of the Pb 4*f* regions as a function of increasing Pb coverage on Ru(0001) at room temperature. The Pb 4*f*_{7/2} peak shifts from a BE of 136.8 eV at 0.2 ML coverage to 137.1 eV at 6 ML. The effect of Pb coverage on the Pb 4*f*_{7/2} peak position is displayed in Fig. 4, where the Pb 4*f*_{7/2} BE is plotted as a function of Pb coverage. The Pb 4*f*_{7/2} BE increases almost linearly with coverage up to one monolayer. Since the Pb atoms in the submonolayer range grow two-dimensionally, the BE changes may reflect a coordination or adsorption site dependence of the Pb 4*f* core level BE. The Pb 4*f*_{7/2} BE, after completion of the first layer of Pb, is only 0.1 eV lower than that of bulk Pb. After completion of a monolayer, only slight changes in the

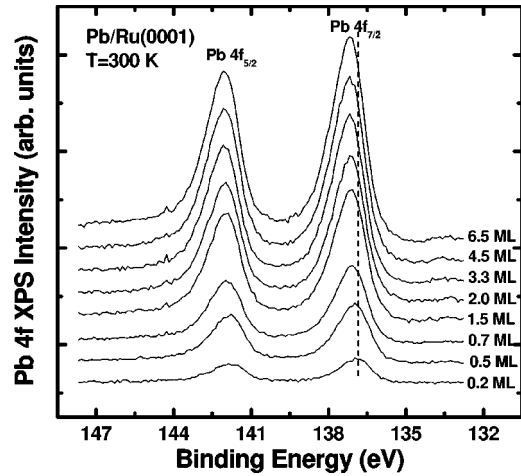


FIG. 3. Effect of Pb coverage on the Pb 4*f* XPS spectra of Pb/Ru(0001).

BE are apparent, with the BE approaching the limiting value of 137.1 eV at coverages > 2 ML. Overall, the XPS data show very little ($+0.3$ eV) BE shift as a function of coverage. Coverages larger than ~ 2 ML show no changes in peak position, consistent with a short-range electronic interaction between Pb and Ru(0001). Furthermore, the Ru 3*d* region of the Pb/Ru(0001) was also monitored at various Pb coverages (not shown) with no apparent change in line shape or peak positions; only a decrease in intensity with increasing Pb coverage was observed.

In order to investigate the thermal stability of the Pb/Ru(0001) system, Pb films were vapor deposited at room temperature, and spectra collected at room temperature after annealing the sample at a specified temperature for 2 min. The maximum annealing temperature was chosen as 500 K because no lead atoms desorb until ~ 550 K, as shown in Fig. 2. Figure 5 shows the effect of annealing on the Pb 4*f* and Ru 3*d* features for 7-ML Pb/Ru(0001). Annealing to 500 K shifted the Pb 4*f*_{7/2} peak by -0.2 eV from the peak position at 300 K whereas the Ru 3*d*_{5/2} feature showed no noticeable change. In Fig. 6, the binding energy of the Pb 4*f*_{7/2}

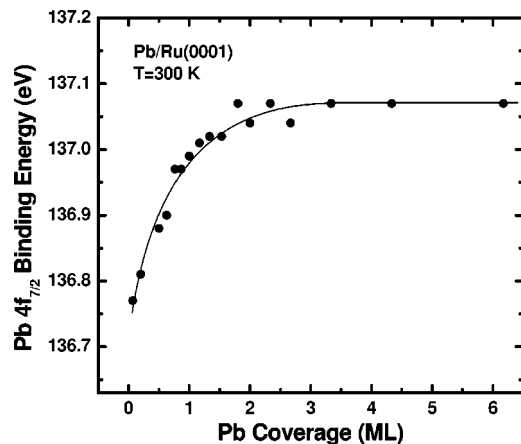


FIG. 4. Plot of Pb 4*f*_{7/2} XPS BE of Pb/Ru(0001) as a function of Pb coverage (film thickness). The solid line is drawn to guide the eye.

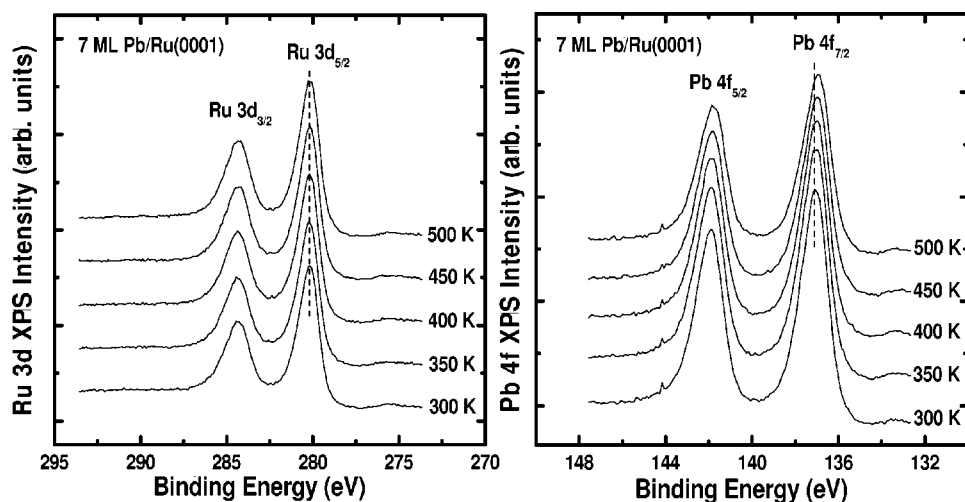


FIG. 5. Effect of annealing temperature upon the Pb 4*f* and Ru 3*d* XPS features for 7-ML Pb on Ru(0001).

peak position along with the Pb 4*f*/Ru 3*d* intensity ratio is plotted as a function of the annealing temperature for three coverages of Pb (1.3, 2.8, and 7 ML). For $\theta_{\text{Pb}}=1.3$ ML, annealing produces no significant change in the Pb 4*f* and Ru 3*d* intensity ratios or the Pb 4*f*_{7/2} BE. Annealing 7-ML Pb films from 300 to 500 K produces significant change in the Pb 4*f*/Ru 3*d* intensity ratio and a relatively small shift in the Pb 4*f*_{7/2} BE peak position (-0.2 eV). The changes for $\theta_{\text{Pb}}=2.8$ ML are intermediate between those for $\theta_{\text{Pb}}=1.3$ and 7 ML. The overall trend in Fig. 6 indicates that the degree of clustering upon annealing of Pb/Ru(0001) increases with Pb coverage, leaving a large fraction of the first monolayer exposed, as reported previously.²⁵⁻²⁷

Figures 7 and 8 show the Pb 4*f* region during progressive Pb vapor deposition on Pd(111) at 300 K. For comparison, the Pb thin films were prepared following the same procedure as that used for Pb/Ru(0001). At $\theta_{\text{Pb}}=0.2$ ML, the Pb 4*f*_{7/2} feature is centered at 136.6 eV; at $\theta_{\text{Pb}}=1.0$ ML, the Pb 4*f*_{7/2} peak is at 137.0 eV and at $\theta_{\text{Pb}}=4.3$ ML, 137.1 eV. The

total shift in Pb 4*f*_{7/2} binding energy changes ~ 0.55 eV from 0.07 ML to the multilayer region. Overall, at low coverage (< 2 ML) the Pb 4*f*_{7/2} BE is smaller than the bulk value and continuously shifts, finally reaching the bulk value at ~ 2 ML (see Fig. 8). The full width half maximum (FWHM) of the Pb 4*f*_{7/2} feature broadens slightly from 1.4 eV at 0.2 ML to 1.5 eV at 4.33 ML.

Figures 9 and 10 display the Pd 3*d* region of the XPS spectra as a function of Pb deposition and the coverage dependence of the Pd 3*d*_{5/2} BE. In contrast to the Ru 3*d* BE in the Pb/Ru(0001) system, the Pd 3*d* BE shows significant change. With an increase in the Pb coverage, the Pd 3*d*_{5/2} peak shifts continuously to high binding energy, reaching $+0.8$ eV at $\theta_{\text{Pb}}=4.3$ ML. The changes in the Pb 4*f*_{7/2} and Pd 3*d*_{5/2} BEs at room temperature are consistent with and appear to indicate that Pb alloys with Pd(111) (denoted Pb_{1-x}Pd_x/Pd(111)). As shown in Fig. 1, the Pb 4*f* intensity changes are also consistent with alloy formation between Pb and Pd. It is noteworthy as well that in Fig. 9, the position and intensities of the Pd 3*d*_{3/2} satellites relative to the main peak strongly depend on the Pb coverage, as seen in other Pd alloys.^{28,29} It may also be suggested that this XPS data, in particular the Pb and Pd BE shifts, are due to an “interdif-

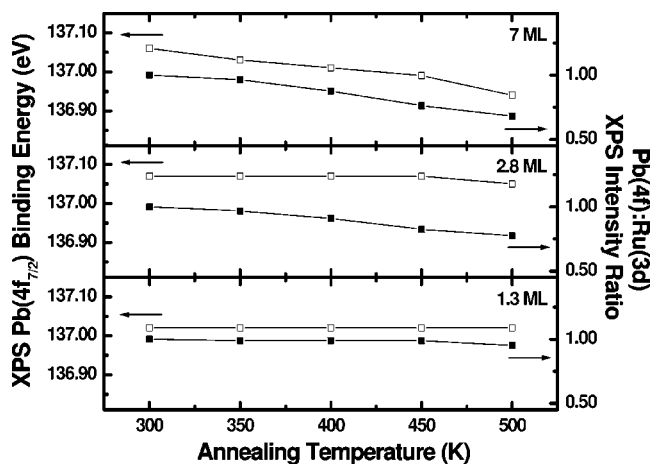


FIG. 6. Variation of the Pb 4*f*_{7/2} XPS peak position and of the Pb 4*f*/Ru 3*d* XPS intensity ratio as a function of annealing temperature for 1.3-, 2.8-, and 7-ML coverages of Pb on Ru(0001). The XPS intensity ratios are normalized to 1 at 300 K in order to be able to compare the temperature changes found for different Pb coverages.

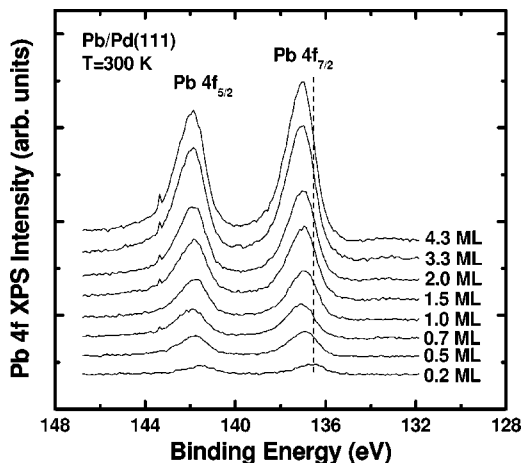


FIG. 7. Effect of Pb coverage on the Pb 4*f* XPS spectra of Pb/Pd(111).

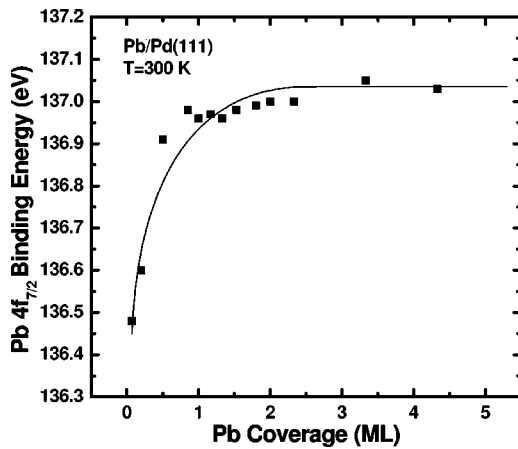


FIG. 8. Plot of Pb $4f_{7/2}$ XPS BE of Pb/Pd(111) as a function of Pb coverage (film thickness). The solid line is a guide for the eye.

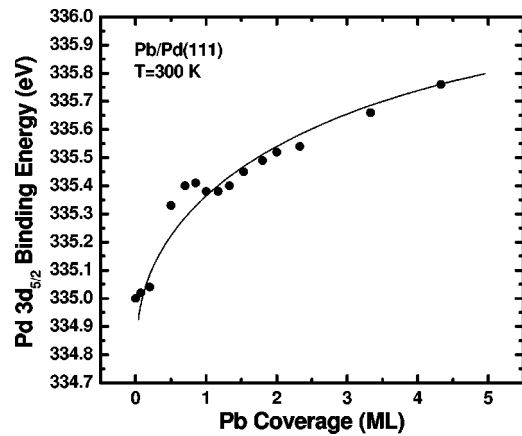


FIG. 10. Plot of Pd $3d_{5/2}$ XPS BE of Pb/Pd(111) as a function of Pb coverage (film thickness). The solid line is a guide for the eye.

fusion” of Pd with the Pb overlayer but this interdiffusion may be viewed as a kind of alloy formation. It is, however, preferable to use the description of alloy formation rather than the less well defined notion of interdiffusion.

Figure 11 illustrates the x-ray induced Auger transition of the Pd ($M_{4,5}VV$) features at $\theta_{Pb}=2.8$ ML for Pb/Pd(111). The lineshapes of the Pd ($M_{4,5}VV$) and their kinetic energies show noticeable changes upon Pb deposition compared to the corresponding values for the clean surface. The M_5VV and M_4VV doublet structure is well defined and the peak positions of the M_5VV and M_4VV features shift toward lower energy by ~ 0.5 eV. Annealing of the system from 300 K, the temperature at which the Pb was deposited, up to 500 K produces no significant changes either in the lineshapes or in the kinetic energies of the Auger spectra. Goetz *et al.*¹² have studied the properties of bimetallic depositions of Pd and Pb on alumina supports by several methods including Fourier transform infrared, XPS, Auger, and other spectroscopies. Based on the ensemble of the data that they obtained, Goetz *et al.*¹² concluded that Pb-Pd alloys were formed. In passing from monometallic Pb to the Pb-Pd al-

loys, they report similar lineshape modifications for the Pd M_{VV} Auger spectra to those reported here. This similarity can be taken as evidence that Pb-Pd alloys are also formed in our case for the deposition of Pb on Pd(111). Still further evidence for alloy formation can be obtained from comparing our Pd Auger spectra for Pb/Pd(111) with those for Cu/Pd(111).⁶ The Pd $M_{4,5}VV$ lineshapes shown in Fig. 11 are quite different from those of Cu/Pd(111),⁶ where the Pd $M_{4,5}VV$ features become less pronounced and featureless with increasing Cu coverage. This sharp contrast can be interpreted to indicate that while for Cu/Pd(111), the Cu forms an overlayer on Pd without significant mixing or interdiffusion, i.e. without alloying, for the case of Pb/Pd(111), a Pb-Pd alloy is formed.

The evolution of the Auger and photoemission spectra of Pd implies a strong interaction between Pb and Pd upon alloying. In addition to the rigid-band shift of ~ 0.5 eV to lower energy, the FWHM of the auger transition decreases by $\sim 10\%$. The observed changes in the $M_{4,5}VV$ bands are consistent with a charge transfer from Pd \rightarrow Pb.

IV. DISCUSSION

The growth modes of one metal evaporated onto another are governed by the surface free energies, strain energies,

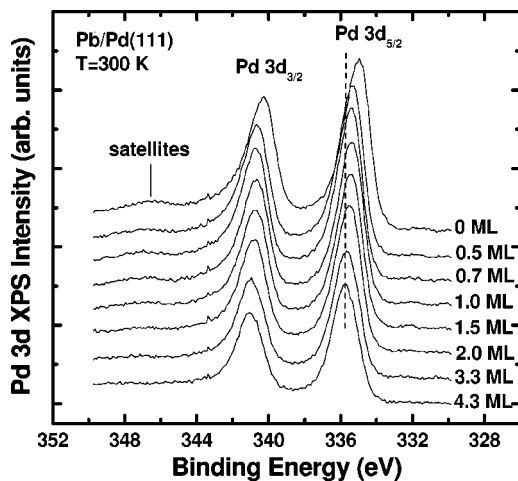


FIG. 9. Effect of Pb coverage on the Pd $3d$ XPS spectra of Pb/Pd(111), including Pd $3d$ satellites.

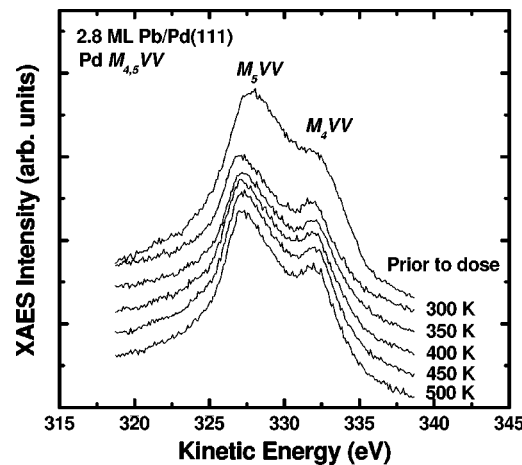


FIG. 11. Effect of coverage and annealing temperature upon Pd ($M_{4,5}VV$) position and line shape for 2.8 ML Pb on Pd(111).

and kinetics. Thermodynamically the growth modes of binary systems are determined by the surface free energies of the substrate (γ_s), the adlayer (γ_a), and the interface energy (γ_i).³⁰ Generally, if the interface energy, γ_i , is less than zero, the system is stabilized by intermixing, maximizing the interface between the adsorbate and the substrate atoms.³¹ However, typically the interface energy γ_i is not known. In addition, the strain energy due to the atomic size mismatch (or the lattice constant mismatch) between the adlayer and the substrate atoms can also induce intermixing in the bulk or at the surface.³²⁻³⁴ Although the Pb surface free energy (0.600 Jm^{-2}) is much smaller than that of Pd (2.050 Jm^{-2}),³⁵ alloys of Pb-Pd contain a number of stoichiometric phases as well as solid solutions.²¹ There is also a large lattice mismatch between Pb and Pd, $\sim 27\%$ [for fcc Pb, $a_{\text{Pb}} = 0.495 \text{ nm}$, for fcc Pd, $a_{\text{Pd}} = 0.389 \text{ nm}$ (Ref. 36)]. Based on the above considerations then, Pb on Pd should intermix, driven either by strain considerations or by bulk alloy formation. For Cu-Pd, which is miscible in the bulk, Cu alloys with Pd when Pd is deposited as an overlayer on a Cu surface.³⁷⁻³⁹ For an immiscible system like Pb on Ru, where surface free energies for Pb and Ru are 0.600 and 3.050 Jm^{-2} , respectively,³⁵ Pb is anticipated to grow in a 2D mode. However, for Pb and Ru, the lattice mismatch is 83% [for hcp Ru, $a_{\text{Ru}} = 0.271 \text{ nm}$ (Ref. 36)], which can induce strain in the overlayer Pb films. This strain energy, if sufficiently large, could cause the growth of three-dimensional clusters after the first monolayer. Pb deposited on other refractory metal surfaces, such as Mo (Ref. 40) and W,⁴¹ follows the Stranski-Krastanov growth mode.

It is well known that the formation of a mixed-metal bond induces perturbations in the electronic properties of the bonded metals.^{3-6,42,43} To compare the core level binding energy of the Pb monolayer with that of the multilayer, it is necessary to take into account the core level shifts of the surface atoms with respect to the bulk core level shifts in the multilayer spectra. To our knowledge, SCLS's of Pb surfaces, either theoretical or experimental, have not been reported.

One effect which leads to core level BE shifts is the transfer of charge between atoms. It is possible to relate the shifts of core level BEs in bimetallic surfaces to an effective charge transfer (CT) between the different metal atoms.³ However, there is strong evidence that other initial state electronic structure properties contribute to core level BE shifts and may well be more important than CT effects (see, for example, Ref. 7 and references therein), thus one should be cautious when using a relationship which directly relates the core level BE shifts, ΔBE , to changes in the effective charge, ΔQ , of an atom. The relationship $\Delta BE \propto \Delta Q$ may neglect other important factors. It is, however, worthwhile to examine the possible effects of charge transfer, especially in the Pb-Ru bimetallic systems. The atomic configuration of Ru and Pd, $[\text{Kr}]4d^7 5s^1$ and $[\text{Kr}]4d$,¹⁰ respectively, show that the $4d$ level will be at or near the Fermi level in condensed systems. For Pb, with configuration $[\text{Xe}]4f^{14} 5d^{10} 6s^2 6p^2$, the $5d$ should be well below E_F . The direction of the charge transfer should be from Pd to Pb or from Ru to Pb,³ since Pd and Ru have a higher density of occupied states near E_F .

For adsorbate metal atoms, such as Pb on Ru(0001), it is reasonable to expect that the effective charge on the Pb might change as a function of coverage of the Pb. For the case of alkali metals on metal surfaces, the traditional view is that the alkali metal is largely ionic at low coverage and becomes essentially neutral as coverage approaches a monolayer or more.⁴⁴ Pacchioni and Bagus⁴⁵ have shown that the core level binding energies of adsorbed K/Cu increase by $\sim 1.6 \text{ eV}$ from a case where the adsorbed alkali is positively charged, K^+ , to one where the K is essentially neutral, K^0 . This shift is consistent with observed coverage dependent shifts of the K $3p$ BE of $\sim 1 \text{ eV}$ for K/Ag (Ref. 46) and K/Ru.⁴⁷ For the case of Pb on Ru(0001), one can speculate that Pb is negatively charged at low coverages and essentially neutral at higher coverages of $\theta \geq 1 \text{ ML}$. As one goes from a negatively charged Pb adsorbate to a neutral adsorbate, the charging contributions lead to a core level BE shift to higher energy. This is consistent with the BE shifts observed for the $4f_{7/2}$ core level for Pb/Ru(0001) of $+0.3 \text{ eV}$. However, this shift cannot be definitively assigned to CT without further, preferably independent, information.

Information on the ionicity of an adsorbate can be obtained from the frustrated translational vibrations of the adsorbate normal to the surface.^{45,48,49} The intensity of these vibrations often depends on the square of the dynamic dipole moment, $e^* = d\mu/dz$,^{50,51} which is large for an ionic and small for a covalently bonded adsorbate.⁴⁵ Similar vibrational measurements are, in principle, possible for Pb on Ru and the measured values of e^* could indicate whether the Pb-Ru bond has significant ionic character.

There are aspects of the Pb-Ru interaction that may not be fully consistent with a high degree of effective anionic character for Pb adsorbates at low coverage. First, the Pb desorption energies change by less than 0.1 eV between 0.13 and 1 ML Pb coverage on Ru(0001). This small change in bond energy is consistent with a similar character of the Pb-Ru bond at both low and high coverages and would argue against a significant anionic character for Pb even at low coverages. The Pauling electronegativities of Pb, Ru, and Pd are reasonably similar with the values for Pd and Ru of ~ 2.2 and for Pb of ~ 2.3 ,⁵² although earlier work gave values for Pb of 1.8 and for Pd and Ru of 2.0 ,⁵³ which are also reasonably close for all three metals. These similar values suggest that CT from Pd or Ru to Pb would be small and the bonding might be best viewed as a polarized covalent bond between Pb and Ru or Pd. In this case, it may be more appropriate to view the bonding in terms of hybridization or rehybridization.^{4,7} Indeed, as will be discussed later, hybridization can make a significant contribution to core level BE shifts. Previous studies indicate that in some bimetallic systems rehybridization localizes electron density in the region of the bimetallic bond.⁵⁴ Furthermore, studies of the near edge x-ray absorption structure for a series of Pd-Ag alloys indicate that the hybridization in the alloys is different from that in the pure metals.⁵⁵

In order to investigate the possible role of hybridization of Pb atoms, it is necessary to determine the levels that may be involved in hybridization. For bulk Pb, the $5d$, $6s$, and $6p$ bands have been shown to be energetically well-separated.⁵⁶

The ground-state configuration for Pb is $[\text{Xe}]4f^{14}5d^{10}6s^26p^2$, where the valence band structure of Pb is dominated by the $6s$ and $6p$ bands. The $6p$ band is near the Fermi level, the $6s$ band, ~ 3 eV below the $6p$ band, and the $5d$ electrons, ~ 10 eV below the $6s$ band. Therefore, the band structure of Pb differs appreciably from that of the $3d$ and $4d$ transition metals where the d and the s - p bands overlap with significant hybridization.⁵⁶ The distinction between the band structures of Pb and of transition metals is important because d to sp hybridization is known to lead to core level BE shifts.⁸ For example, the sign of the SCLS at Cu surfaces arises because of the different extent of the $3d \rightarrow 4sp$ hybridization for bulk and surface atoms.⁸ However, $s \rightarrow p$ hybridization, which occurs for simple metals, can also lead to core level BE shifts. This has been shown to be important for the BE shifts in Al,^{8,57} and it seems likely that it would also be true for Pb.

In order to have a foundation for the analysis of core level BE shifts, the mechanisms responsible for these shifts will be reviewed following the work in Refs. 7, 8, and 57. In this work, the mechanisms are divided into initial state effects where shifts arise because of the chemical bonding, including charge transfer, and into final state effects that take into account BE shifts due to differential screening of the core hole. There are two initial state mechanisms which make canceling contributions to shifts of the core level BEs. The first arises from hybridization. Since electronic charge *after* hybridization is more diffuse, the initial state BE's are larger than they were before hybridization. This mechanism was first pointed out by Mason⁵⁸ to explain the core level BE shifts in metal clusters as a function of cluster size. It is reasonable to expect that hybridization, linked as it is to the strength of the chemical bonding of the hybridized atom, will depend on the coordination, or the number of nearest neighbors, of the atom.^{7,8,57} For metal clusters, it has also been shown that the extent of the hybridization, especially for the relatively contracted nd levels of transition metals, also depends on the bond distances, or the effective lattice constant, for metal clusters.⁵⁹ For shorter bond lengths, the hybridization is greater than for longer bond lengths. This is chemically logical since a reduction of the bond length increases the overlap of d orbitals on neighboring atoms and favors involvement of these orbitals in the formation of covalent chemical bonds. Transmission electron microscopy studies⁶⁰ have shown that there is a modest increase in bond length with cluster size for metal clusters on inert supports going to the limit of the bulk lattice constant for very large clusters. Theoretical analysis has related this lattice strain in small clusters to shifts to higher BE due to the different, larger extent of hybridization in the small clusters.⁵⁹ The second initial state mechanism that contributes to BE shifts is the "conduction band," or environmental, charge density. When an atom is in an environment where there is a greater amount of charge density that surrounds the atomic core, there is a shift of core level BEs to lower energy. This mechanism was first pointed out in connection with the BE shifts of metal clusters by Parmigiani *et al.*⁶¹ For this mechanism, the BE shift is also related to the coordination of the core ionized atom. For atoms with a higher coordination, the environmen-

tal charge density is larger and it contributes a larger environmental shift to lower BE. Note that this is the opposite direction as the change in BE shifts due to the hybridization mechanism where there is a larger shift to higher BE with increasing hybridization. The contributions of these two initial state mechanisms to core level BE shifts are canceling. Hybridization increases BEs and the "conduction band" charge density lowers BEs. With suitable methods of electronic structure theory,^{7,8,62} it is possible to decompose the contributions of these two initial state mechanisms as well as to separate the final state contributions due to relaxation in response to the core hole. For the Cu(100) SCLSs, we have made this decomposition for the $2s$ BE following the methods of Bagus *et al.*^{7,8} The SCLS for the $2s$ BE should be similar to the $2p_{3/2}$ BE SCLS that has been measured to be ~ 0.25 eV toward higher BE for a bulk atom.⁶³ The greater density of conduction band charge density around a 12-fold coordinated bulk atom than an eightfold coordinated (100) surface atom contributes -0.50 eV to the SCLS toward a smaller BE for a bulk atom. On the other hand, the larger extent of the $3d$ hybridization for a bulk than for a surface atom contributes $+1.24$ eV to the SCLS. The cancellation of these two effects leads to a net initial state SCLS of $+0.74$ eV. There is a final state relaxation that is larger for a bulk atom by 0.26 eV than for a surface atom. This differential relaxation further reduces the SCLS.

It is common to think of the hybridization as involving promotion from relatively compact d levels. However, it is also possible to have hybridization of ns electrons into np and other bonding levels, where n denotes the outermost shell of the atom. For example, for a bulk fcc Cu atom, hybridization of the $3d$ electrons contributes an increase of ~ 3.5 eV to the core level BEs over the value of the BE when the Cu $3d$ orbitals are fixed,⁶² frozen, to have their atomic character and hybridization is not allowed. However, for a bulk fcc Al atom, hybridization of the $3s$ electrons also contributes ~ 3.5 eV to increase the Al core level BEs.⁵⁷ Clearly, hybridization of ns levels in simple metals like Al, with atomic configuration $\dots 3s^23p^1$, or Pb, with atomic configuration $\dots 5d^{10}6s^26p^2$, cannot be neglected. Indeed, a simple atomic analysis shows that hybridization in Pb can be expected to be of similar magnitude as for Al. For the Al and Pb atoms, we compare the initial state core level BE shifts between the atom in its ground state and a state where an ns electron is promoted, or hybridized, to the np shell. For Al, the configurations are $3s^23p^1$ and $3s^13p^2$ and the shift is considered for the $2p$ BE; for Pb, the configurations are $6s^26p^2$ and $6s^16p^3$ and the shift is considered for the $4f$ BE. Hartree-Fock atomic wave functions are computed for the average of the multiplet couplings for each of these configurations⁶⁴ and the initial state BE shift, ΔBE , is obtained by taking the differences of the core-level orbital energies for the two configurations considered for each atom.^{65,66} The BE shift for Al is $\Delta\text{BE}(2p) = +1.9$ eV while for Pb, it is $\Delta\text{BE}(4f) = +1.4$ eV. Thus for the analysis of the initial state BE shifts of Pb, it is necessary to take into account hybridization as well as the environmental conduction band charge density. As we noted above, the magnitudes of both the hybridization and the environmental charge den-

sity initial state shifts increase with increasing coordination of the core ionized atom. These considerations suggest an interpretation for the origin of the 0.3 eV increase of Pb $4f_{7/2}$ BEs with increasing coverage of Pb on Ru(0001) (see Figs. 3 and 4). It is consistent that the contribution to this BE shift arising from the hybridization of the Pb $6s$ electrons dominates that arising from the environmental charge density. However, it should be recalled that this discussion has not invoked possible contributions from charge transfer or from final state effects. The possible contributions of charge transfer have been discussed above; brief comments on final state effects follow.

Final state effects on the core level BE's arise because of the relaxation of the "passive" electrons in response to the presence of the core ionized atom. This relaxation is often described as a "screening" of the core hole. The absolute value of the final state relaxation energy is quite large,^{7,8,67,68} easily on the order of tens of eV, and it must be taken into account to obtain accurate values of the BEs. However, for BE shifts, it is only the differential final state relaxation energy that is important. It is reasonable that the relaxation energies of ionized Pb atoms would not depend strongly on the Pb coverage. One may regard the screening charge as arising dominantly from the reservoir of conduction band charge in the Ru(0001) substrate and, in this case, the relaxation will not depend on Pb coverage. Another way of saying this is that the final state screening in a metallic system is long range and does not depend strongly on the immediate environment of the core ionized atom. Of course, the response of a Pb atom to the presence of a core hole on a nearby ionized Pb atom may be different from the response of a Pd atom to this core hole. Hence, the final state relaxation energy for a Pb core hole in an atom at the surface of a Pb crystal may be different from the relaxation energy for a core hole in a Pb atom adsorbed on the surface of a crystal of another metal. To our knowledge, estimates of the magnitude of this effect are not available.

Chadwick and Karolewski⁶⁹ studied the adsorption of Pb on polycrystalline Pd including measurements of core level BE shifts and concluded that Pb-rich intermediate alloy phases, PdPb₂ and or PdPb, were formed. There are significant similarities between their XPS results and our results; however, there are also differences, in particular for the magnitudes of the BE shifts with Pd coverage. They found, as we have also found, that the Pb $4f_{7/2}$ BE converged to the value for bulk Pb at ~ 2 ML coverage. Moreover, our measurement of the broadening of the Pb XPS peak as a PbPd alloy formed was ~ 0.05 eV (see Fig. 7), and this is consistent with the value of 0.04 reported in Ref. 69. On the other hand, they⁶⁹ report that the Pb $4f_{7/2}$ BE increase between coverages of 0.1 to 2 ML was ~ 0.16 eV, considerably smaller than the increase of 0.55 eV that we found; see Fig. 8. Similarly, the increase of the Pd $3d_{5/2}$ BE of ~ 0.8 eV at a coverage of 4.33 ML (see Fig. 10), is significantly larger than 0.5 eV for Pb overlayers reported in Ref. 69. Furthermore, Chadwick and Karolewski⁶⁹ used data on alloy heats of formation to estimate core level BE shifts in dilute Pb-Pd alloys; these estimates are based on the use of Born-Haber cycles.⁷⁰ They obtained estimated values of a +1.5-eV Pd

BE shift for dilute Pd in Pb and a -0.3 eV Pb shift for dilute Pb in Pd. However, we urge caution for the applicability of these calculated estimates since they are not fully consistent neither with our XPS data for Pb/Pd nor with the data of Chadwick and Karolewski.⁶⁹ Both our work and that of Ref. 69 give evidence that PbPd alloys are formed at the interface when Pb is deposited on Pd. However, it is not possible to determine an accurate alloy composition without additional data. In particular, studies of the electronic properties of well-defined or amorphous intermetallic compounds of the type Pb_{1-x}Pd_x would allow the specific nature of the alloys or compounds formed at the interface to be addressed.

There is one further study of Pb deposited on metals that may be relevant to the present work. For Pb deposited on polycrystalline Pt, the Pb $4f$ binding energy was reported to change very little with Pb coverage.⁷¹ However, a slight increase in the linewidth with the Pb coverage was observed, suggesting alloy formation between Pb and Pt. It was suggested that the absence of a Pb $4f$ shift may be due to the compensation of initial and final state effects.⁷¹ It is possible to try to relate the saturation of the Pb $4f_{7/2}$ BE at ~ 2 ML to the short-range interaction between Pb and Ru, and to bulk-like Pb formation upon clustering.

Clearly, further experimental and theoretical work is required in order to be able to relate the Pb core level BE shifts reported in this paper to the nature of the electronic structure of the interaction of adsorbed Pb atoms with each other and with the substrate. For example, it would be useful to know the SCLS on Pb surfaces in order to compare this with our measured shift for the lowest coverages of Pb/Ru(0001) of -0.3 eV for the Pb $4f_{7/2}$ BE taken with respect to bulk Pb. It is also important to understand the significance of the rapid convergence of the Pb $4f_{7/2}$ BE to its bulk value which we have shown occurs at only 2-ML coverage for Pb/Ru(0001); see Fig. 4. However, our experimental results establish the extent and the main features of these BE shifts and indicate the additional information that is needed. Furthermore, calculations that decompose the total BE shifts into contributions from the various initial and final state mechanisms will be of considerable value. These calculations will permit the interpretation of these shifts in terms of the physical and chemical environments of the core ionized atoms. However, the theoretical analysis which we have made based on previous studies of the origin of BE shifts in single metal systems has provided extremely valuable information. In particular, it is established that several mechanisms make important contributions to the observed BE shifts; furthermore, these contributions are almost certainly canceling.

V. CONCLUSIONS

The interaction of ultrathin Pb films with Ru(0001) and Pd(111) was studied by XPS and TDS. The adsorption of Pb on Ru(0001) and Pd(111) at room temperature leads to varying growth modes: the former, to cluster formation after the first monolayer completion; the latter to alloy formation, governed by energetics and/or strain of the systems.

XPS results show that the Pb $4f_{7/2}$ BE increases slightly with Pb coverage on Ru(0001), approximately +0.3 eV from

$\theta_{\text{Pb}}=0.07$ ML to $\theta_{\text{Pb}}=6$ ML. However, the Pb $4f_{7/2}$ BE for the first layer of Pb is only 0.1 eV lower than that of bulk Pb; by $\theta_{\text{Pb}}\sim 2$ ML, the Pb $4f_{7/2}$ BE reaches the Pb bulk level. Upon annealing to 500 K, XPS results show the Pb adsorbates cluster on Ru(0001), depending upon the Pb initial coverages.

In the case of Pb adsorption on Pd(111), analysis of the core level shifts from XPS shows that the Pd $3d_{5/2}$ BE continuously increases with Pb coverage, approximately +0.8 eV at $\theta_{\text{Pb}}=4.3$ ML. However, the Pb $4f_{7/2}$ BE readily saturates at the bulk value at a coverage of ~ 2 ML, while the Pb $4f_{7/2}$ BE of $\theta_{\text{Pb}}=0.07$ ML is 0.55 eV lower than that of $\theta_{\text{Pb}}=2$ ML. In the case of Pb/Pd alloys, the lineshape and position of the Pd Auger ($M_{4,5}VV$) features show significant changes at $\theta_{\text{Pb}}=2.8$ ML. Upon annealing to 500 K, no further noticeable changes were observed for the Pd ($M_{4,5}VV$) features.

Further studies, both theoretical and experimental, are re-

quired to make a definitive analysis of the relative importance of the various initial and final state contributions to the core level binding energy shifts. However, from the analyses which we have made, it is clear that the origin of the observed BE shifts is not likely to be due to a single mechanism. The most likely case is that the BE shifts are the result of canceling contributions from more than one mechanism. Thus, it is necessary to be very cautious about attempts to relate these BE shifts to a single origin; e.g., charge transfer effects.

ACKNOWLEDGMENTS

This work was supported by the Department of Energy, the Office of Energy Research, Division of Chemical Sciences, the Robert A. Welch Foundation, and the BP Chemical Company.

*Author to whom correspondence should be addressed.

- ¹J. H. Sinfelt, *Bimetallic Catalysts: Discoveries, Concepts, and Applications* (Wiley, New York, 1983); V. Ponc, Adv. Catal. **32**, 149 (1983).
- ²C. T. Campbell, Annu. Rev. Phys. Chem. **41**, 775 (1990).
- ³J. A. Rodriguez and D. W. Goodman, Science **257**, 897 (1992).
- ⁴J. A. Rodriguez, Surf. Sci. Rep. **24**, 223 (1996).
- ⁵D. W. Goodman, J. Phys. Chem. **100**, 13090 (1996); Surf. Sci. **299/300**, 837 (1994).
- ⁶G. Liu, T. P. St. Clair, and D. W. Goodman, J. Phys. Chem. B **103**, 8578 (1999).
- ⁷P. S. Bagus, F. Illas, G. Pacchioni, and F. Parmigiani, J. Electron Spectrosc. Relat. Phenom. **100**, 215 (1999).
- ⁸P. S. Bagus, C. R. Brundle, G. Pacchioni, and F. Parmigiani, Surf. Sci. Rep. **19**, 265 (1993).
- ⁹L. L. Hegedus and J. J. Gumbleton, CHEMTECH **10**, 630 (1980).
- ¹⁰J. P. Boitiaux, J. Cosyns, M. Derrien, and G. Léger, Hydrocarbon Process. **64**, 51 (1985).
- ¹¹V. H. Sandoval, C. E. Gigola, Appl. Catal., A **148**, 81 (1996).
- ¹²J. Goetz, M. A. Volpe, A. M. Sica, C. E. Gigola, and T. Touroude, J. Catal. **167**, 314 (1997).
- ¹³H. R. Aduriz, C. E. Gigola, A. M. Sica, M. A. Volpe, and R. Touroude, Catal. Today **15**, 459 (1992).
- ¹⁴R. M. Ferullo, R. Touroude, and N. J. Castellani, Surf. Rev. Lett. **4**, 621 (1997).
- ¹⁵J. Stachurski and J. M. Thomas, Catal. Lett. **1**, 67 (1988).
- ¹⁶W. Palczewska, A. Jabłoński, Z. Kaszukur, G. Zuba, and J. Wernisch, J. Mol. Catal. **25**, 307 (1984).
- ¹⁷R. Schlögl, K. Noack, H. Zbinden, and A. Reller, Helv. Chim. Acta **70**, 627 (1987).
- ¹⁸T. Tsujino, S. Ohigashi, S. Sugiyama, K. Kawashiro, and H. Hayashi, J. Mol. Catal. **71**, 25 (1992).
- ¹⁹T. Mallat and A. Baiker, Appl. Catal., A **79**, 41 (1991); T. Mallat, A. Baiker, and J. Patscheider, *ibid.* **79**, 59 (1991).
- ²⁰H. Hayashi, S. Sugiyama, Y. Katayama, K. Kawashiro, and N. Shigemoto, J. Mol. Catal. **91**, 129 (1994).
- ²¹T. B. Massalski, H. Okamoto, P. R. Subramanian, and L. Kacprzak, *Binary Alloy Phase Diagrams* (ASM International, Materials Park, OH, 1990).
- ²²J. E. Parmeter, X. Jiang, and D. W. Goodman, Surf. Sci. **240**, 85 (1990).
- ²³P. A. Redhead, Vacuum **12**, 203 (1962).
- ²⁴A. R. Miedema and J. W. F. Dorleijn, Surf. Sci. **95**, 447 (1980).
- ²⁵J. A. Rodriguez, R. A. Campbell, and D. W. Goodman, J. Phys. Chem. **95**, 2477 (1991).
- ²⁶J. E. Houston, C. H. F. Peden, D. S. Blair, and D. W. Goodman, Surf. Sci. **167**, 427 (1986).
- ²⁷B. E. Koel, A. Sellidj, and M. T. Paffett, Phys. Rev. B **46**, 7846 (1992).
- ²⁸F. Bertran, T. Gourieux, G. Krill, M. F. Ravet-Krill, M. Alnot, J. J. Ehrhardt, and W. Felsch, Phys. Rev. B **46**, 7829 (1992).
- ²⁹F. U. Hillebrecht, J. C. Fuggle, P. A. Bennett, Z. Zolnierok, and Ch. Freiburg, Phys. Rev. B **27**, 2179 (1982).
- ³⁰H. Röder, R. Shuster, H. Brune, and K. Kern, Phys. Rev. Lett. **71**, 2086 (1993).
- ³¹E. Bauer, Appl. Surf. Sci. **11/12**, 479 (1982).
- ³²J. W. Cahn, Acta Metall. **9**, 795 (1961).
- ³³R. M. Tromp, Phys. Rev. B **47**, 7125 (1993).
- ³⁴J. Tersoff, Phys. Rev. Lett. **74**, 434 (1995).
- ³⁵F. R. de Boer, R. Boom, W. C. M. Mattens, A. R. Miedema, A. K. Niessen, *Cohesion in Metals: Transition Metal Alloys*, edited by F. R. de Boer and D. G. Pettifor (Elsevier, Amsterdam, 1988).
- ³⁶C. Kittel, *Introduction to Solid State Physics*, 7th ed. (Wiley, New York, 1996), p. 23.
- ³⁷P. W. Murray, I. Stensgaard, E. Lægsgaard, and F. Besenbacher, Phys. Rev. B **52**, R14404 (1995).
- ³⁸P. W. Murray, S. Thorshaug, I. Stensgaard, F. Besenbacher, E. Lægsgaard, A. V. Ruban, K. W. Jacobsen, G. Kopidakis, and H. L. Skriver, Phys. Rev. B **55**, 1380 (1997).
- ³⁹A. Bach Aaen, E. Lægsgaard, A. V. Ruban, and I. Stensgaard, Surf. Sci. **408**, 43 (1998).
- ⁴⁰M. Tikhov and E. Bauer, Surf. Sci. **203**, 423 (1988).
- ⁴¹E. Bauer, H. Poppa, and G. Todd, Thin Solid Films **28**, 19 (1975).
- ⁴²B. Hammer, Y. Morikawa, and J. K. Nørskov, Phys. Rev. Lett. **76**, 2141 (1996).
- ⁴³D. Hennig, M. V. Ganduglia-Pirovano, and M. Scheffler, Phys. Rev. B **53**, 10344 (1996).

- ⁴⁴See, for example, *Physics and Chemistry of Alkali Metal Adsorption*, edited by M. P. Bonzel, A. Bradshaw, and G. Ertl (Elsevier, New York, 1989); T. Aruga and Y. Murata, *Prog. Surf. Sci.* **31**, 61 (1989); H. P. Bonzel, *Surf. Sci. Rep.* **8**, 43 (1987).
- ⁴⁵G. Pacchioni and P. S. Bagus, *Surf. Sci.* **286**, 317 (1993).
- ⁴⁶S. Modesti, C. T. Chen, Y. Ma, G. Meigs, P. Rudolf, and F. Sette, *Phys. Rev. B* **42**, 5381 (1990).
- ⁴⁷M. L. Shek, J. Hrbek, T. K. Sham, and G. Q. Xu, *Phys. Rev. B* **41**, 3447 (1990).
- ⁴⁸S. A. Lindgren, C. Svensson, and L. Walldén, *Phys. Rev. B* **42**, 1467 (1990).
- ⁴⁹P. Rudolf, C. Astaldi, G. Cautero, and S. Modesti, *Surf. Sci.* **251/252**, 127 (1991).
- ⁵⁰H. Ibach and D. L. Mills, *Electron Energy Loss Spectroscopy and Surface Vibrations* (Academic Press, New York, 1982).
- ⁵¹G. Pacchioni and P. S. Bagus, *J. Chem. Phys.* **93**, 1209 (1990).
- ⁵²A. L. Allred, *J. Inorg. Nucl. Chem.* **17**, 215 (1961).
- ⁵³W. Gordy and W. J. O. Thomas, *J. Chem. Phys.* **24**, 439 (1956).
- ⁵⁴J. A. Rodriguez and M. Kuhn, *Chem. Phys. Lett.* **240**, 435 (1995); J. A. Rodriguez, *Surf. Sci.* **303**, 366 (1994); *J. Phys. Chem.* **98**, 5758 (1994); J. A. Rodriguez, R. A. Campbell, and D. W. Goodman, *Surf. Sci.* **307-309**, 377 (1994).
- ⁵⁵I. Coulthard and T. K. Sham, *Phys. Rev. Lett.* **77**, 4824 (1996).
- ⁵⁶K. Würde, A. Mazur, and J. Pollmann, *Phys. Rev. B* **49**, 7679 (1994), and references therein.
- ⁵⁷P. S. Bagus and G. Pacchioni, *Phys. Rev. B* **48**, 15274 (1993).
- ⁵⁸M. G. Mason, *Phys. Rev. B* **27**, 748 (1983).
- ⁵⁹B. Richter, H. Kuhlenbeck, H.-J. Freund, and P. S. Bagus (unpublished).
- ⁶⁰S. A. Nepijko, M. Klimenkov, M. Adelt, H. Kuhlenbeck, R. Schlögl, and H.-J. Freund, *Langmuir* **15**, 5309 (1999); M. Klimenkov, S. Nepijko, H. Kuhlenbeck, M. Bäumer, R. Schlögl, and H.-J. Freund, *Surf. Sci.* **391**, 27 (1997).
- ⁶¹F. Parmigiani, E. Kay, and P. S. Bagus, *J. Electron Spectrosc. Relat. Phenom.* **50**, 39 (1990).
- ⁶²P. S. Bagus and F. Illas, *J. Chem. Phys.* **96**, 8962 (1992); P. S. Bagus, K. Hermann, and C. W. Bauschlicher, Jr., *ibid.* **80**, 4378 (1984).
- ⁶³P. S. Bagus, G. Pacchioni, and F. Parmigiani, *Phys. Rev. B* **43**, 5172 (1991).
- ⁶⁴J. C. Slater, *Quantum Theory of Atomic Structure* (McGraw-Hill, New York, 1960), Vol. II.
- ⁶⁵P. A. Cox, *Mol. Phys.* **30**, 389 (1972).
- ⁶⁶K. Hermann and P. S. Bagus, *Phys. Rev. B* **16**, 4195 (1977).
- ⁶⁷P. S. Bagus, *Phys. Rev.* **139**, A619 (1965).
- ⁶⁸P. S. Bagus, D. Coolbaugh, S. P. Kowalczyk, G. Pacchioni, and F. Parmigiani, *J. Electron Spectrosc. Relat. Phenom.* **51**, 69 (1990).
- ⁶⁹D. Chadwick and M. A. Karolewski, *Surf. Sci.* **126**, 41 (1983).
- ⁷⁰B. Johansson and N. Mårtensson, *Phys. Rev. B* **21**, 4427 (1980).
- ⁷¹T. T. P. Cheung, *Surf. Sci.* **177**, L887 (1986).